

Evolution of blue E/S0 galaxies from $z \sim 1$: merger remnants or disk-rebuilding galaxies?

M. Huertas-Company^{1,2,3}, J. A. L. Aguerri⁴, L. Tresse⁵, M. Bolzonella⁶, A. M. Koekemoer⁷, and C. Maier⁸

¹ ESO, Alonso de Cordova 3107, Casilla 19001, Vitacura, Santiago, Chile
e-mail: mhuertas@eso.org; marc.huertas@obspm.fr

² GEPI – Observatoire de Paris, Section de Meudon, 5 Place Jules Janssen, 92190 – Meudon, France

³ University of Paris Denis Diderot, 75205 Paris Cedex 13, France

⁴ Instituto de Astrofísica de Canarias, C/ vía Láctea s/n, 38200 La Laguna, Spain

⁵ LAM-CNRS Université de Provence, 38 rue Frédéric Joliot-Curie, 13388 Marseille Cedex 13, France

⁶ INAF – OA Bologna, via Ranzani 1, 40127 Bologna, Italy

⁷ Space Telescope Science Institute 3700 San Martin Drive, Baltimore MD 21218, USA

⁸ Institute of Astronomy, Swiss Federal Institute of Technology (ETH Hönggerberg), 8093 Zürich, Switzerland

Received 26 August 2009 / Accepted 4 February 2010

ABSTRACT

Context. Studying outliers from the bimodal distribution of galaxies in the color-mass space, such as morphological early-type galaxies residing in the blue cloud (*blue E/S0s*), can help for better understanding the physical mechanisms that lead galaxy migrations in this space.

Aims. In this paper we try to bring new clues to studying the evolution of the properties of a significant sample of blue E/S0 galaxies in the COSMOS field.

Methods. We define blue E/S0 galaxies as objects having a clear early-type morphology on the HST/ACS images (according to our automated classification scheme *GALSVM*) but with a blue rest-frame color (defined by using the SED best-fit template on the COSMOS primary photometric catalogs). Combining these two measurements with spectroscopic redshifts from the zCOSMOS 10k release, we isolated 210 $I_{AB} < 22$ blue early-type galaxies with $M_*/M_\odot > 10^{10}$ in three redshift bins ($0.2 < z < 0.55$, $0.55 < z < 0.8$, $0.8 < z < 1.4$) and studied the evolution of their properties (number density, SFR, morphology, size).

Results. The threshold mass (M_t), defined at $z = 0$ in previous studies as the mass below which the population of blue early-type galaxies starts to be abundant relative to passive E/S0s, evolves from $\log(M_*/M_\odot) \sim 10.1 \pm 0.35$ at $z \sim 0.3$ to $\log(M_*/M_\odot) \sim 10.9 \pm 0.35$ at $z \sim 1$. Interestingly, it follows the evolution of the crossover mass between the early and late type populations (bimodality mass) indicating that the abundance of blue E/S0 is another measure of the downsizing effect in the build-up of the red sequence. There seems to be a turn-over mass in the nature of blue E/S0 galaxies. Above $\log(M_*/M_\odot) \sim 10.8$ blue E/S0 resemble to merger remnants probably migrating to the red sequence on a time scale of ~ 3 Gyr. Below this mass, they seem to be closer to normal late-type galaxies, as if they were the result of minor mergers that triggered the central star formation and built a central bulge component or were (re)building a disk from the surrounding gas in a much longer time scale, suggesting that they are moving back or staying in the blue cloud. This turn-over mass does not seem to evolve significantly from $z \sim 1$ in contrast to the threshold mass and therefore does not seem to be linked with the relative abundance of blue E/S0s.

Key words. galaxies: evolution – galaxies: formation – galaxies: fundamental parameters – galaxies: high-redshift

1. Introduction

It is well-established that there is a clear bimodality of the $z \sim 0$ galaxy distribution in the color-mass/magnitude space. The red sequence (RS) is mostly composed of red, passive early-type galaxies and the blue cloud contains blue, star-forming late-type galaxies. One fundamental point is to understand the mechanisms that drive the building-up of this relation. What are the movements in this color-mass space? How do galaxies move from the blue cloud to the red sequence and vice versa?

The blue cloud and the red sequence are not uniformly distributed in color-mass space. Red galaxies indeed dominate in number at high stellar masses, and the crossover stellar mass between late and early-type galaxies has been called *bimodality mass* (M_b) (e.g. [Strateva et al. 2001](#); [Baldry et al. 2004](#);

[Kauffmann et al. 2006](#); [Faber et al. 2007](#)). Recent high-redshift studies have shown that this bimodality mass has evolved from $M_b \sim 1\text{--}2 \times 10^{11} M_\odot$ at $z \sim 1$ to $M_b \sim 3 \times 10^{10}$ at $z \sim 0$ (e.g. [Bundy et al. 2005](#); [Cimatti et al. 2006](#)). This has been interpreted as another signature of the downsizing effect ([Cowie et al. 1996](#)) in the galaxy formation processes with galaxies moving from the blue cloud to the red sequence at higher masses when we look back in time, even if, as argued by [Cattaneo et al. \(2008\)](#), this interpretation is not always straightforward.

While the *basic* physics behind it has been known since a series of seminal papers published 20–30 years ago (e.g. [Rees & Ostriker 1977](#); [Binney 1977](#); [White & Rees 1978](#); [Blumenthal et al. 1984](#)), a detailed understanding is still in progress, in particular through the works of [Dekel & Birnboim \(2006\)](#) and [Kereš et al. \(2005\)](#). The result is that, to quench the star formation

in an efficient way and to reproduce the mass-dependent transitions, recent semi-analytical models (e.g. De Lucia et al. 2006; Cattaneo et al. 2006) need to use different combinations of AGN feedbacks (e.g. Silk & Rees 1998; Fabian 1999; King 2003; Wyithe & Loeb 2003) and merging (e.g. Hernquist & Mihos 1995; Mihos & Hernquist 1996; Springel et al. 2005b).

From an observational point of view, it becomes interesting to study outliers in the color morphology relation since they can represent objects in transition, and can bring new clues to its origin. As a matter of fact, some recent studies have pointed out that, at $z = 0$, some low mass morphologically defined E/S0s start to appear in the blue cloud (e.g. Bamford et al. 2009; Kannappan et al. 2009; Schawinski et al. 2009). These so-called *blue early type* galaxies have also been found at higher redshift (e.g. Ilbert et al. 2006b; Ferreras et al. 2009).

However, the detailed analysis of blue E/S0 galaxies has just started. At $z = 0$, Kannappan et al. (2009) find a clear dependence on mass of the properties of these objects. They basically identified three mass regimes: above the shutdown mass $M_s \sim 10^{11} M_\odot$ blue-early type galaxies are non-existent (as most of the blue cloud), below the threshold mass ($M_t \sim 10^9$) they become extremely abundant, representing $\sim 20\text{--}30\%$ of all the E/S0 population and between M_s and M_t where the bimodality mass lies, they account for $\sim 5\%$ of the E/S0 population. The nature of the physical processes taking place in these mass regimes seem to be different as well. As a matter of fact, the shutdown mass could be related with the different temperature of the gas accreted by dark matter haloes above and below a critical mass of $\sim 10^{12} M_\odot$ (e.g. Bundy et al. 2005; Cattaneo et al. 2006; Dekel & Birnboim 2006). Blue early-type galaxies in the mass range $M_s < M < M_b$ resemble to merger remnants that are probably moving to the red sequence (Kannappan et al. 2009). Hierarchical formation theories predict indeed that most of the spiral galaxies have undergone a major merger event in the last 8 Gyr. Those mergers between galaxies with a large fraction of gas provoke a short (0.1 Gyr) and strong peak of star formation (e.g. Springel et al. 2005b,a). Mergers do not only change the stellar content of the galaxies but also induce a dramatic change of their morphology. In particular, the disks are suppressed producing a compact morphology that could be associated with an early-type galaxy (Barnes 2002). In contrast, below M_t blue early-type galaxies are likely rebuilding disks and therefore moving to or staying in the blue cloud (Kannappan et al. 2009). Major mergers also induce shock-heated gas winds as well as the formation of a remnant gas halo with a large cooling time and could produce an enriched medium with which a gas disk could be formed (Cox et al. 2004). Recently, some examples of rebuilding disks have also been found in luminous compact blue galaxies (Puech et al. 2007; Hammer et al. 2009). It is interesting that M_t also corresponds with the mass below which galaxies have larger gas reservoirs (Kannappan 2004; Kannappan & Wei 2008).

The next step in the characterization of blue E/S0s is to follow them at higher redshift. As a matter of fact since the transition from the blue cloud to the red sequence is mass-dependent, we expect these different characteristic masses to evolve with look-back time and therefore the properties of blue E/S0s for a given mass as well.

In this work we look for blue E/S0 galaxies, similar to those reported in recent studies in the nearby Universe, between $z \sim 0.2$ and $z \sim 1.4$ in the spectroscopic follow-up of the galaxies detected in the HST/ACS COSMOS field (i.e. the public 10k-bright sample, Lilly et al. 2009). We investigate their observational properties (number density, morphology, size, star-forming rate), compare them with similar galaxies at $z = 0$

(Kannappan et al. 2009; Schawinski et al. 2009) and try to give new clues about their nature and evolution. The paper proceeds as follows: in Sects. 2 and 3 we describe our sample and the methods to obtain physical properties of the galaxies. Section 4 is focused on the definition and characterization of blue early-type galaxies at different redshifts. Finally, in Sect. 5 we discuss the main results and conclusions are given in Sect. 6.

Throughout the paper, we assume that the Hubble constant, the matter density, and the cosmological constant are $H_0 = 70 \text{ km s}^{-1} \text{ Mpc}^{-1}$, $\Omega_m = 0.3$ and $\Omega_\Lambda = 0.7$ respectively. All magnitudes are in the AB system.

2. Dataset and sample selection

We use the public available zCOSMOS 10k sample corresponding to the second release of the zCOSMOS-bright survey (Lilly et al. 2009). The zCOSMOS-bright, aims to produce a redshift survey of approximately 20000 *I*-band selected galaxies ($15 < I_{AB} < 22.5$). Covering the approximately 1.7 deg^2 of the COSMOS field (Scoville et al. 2007) (essentially the full ACS-covered area), the transverse dimension at $z \sim 1$ is 75 Mpc. This second release (DR2) contains the results of the zCOSMOS-bright spectroscopic observations that were carried out in VLT service mode during the period April 2005 to June 2006. 83 masks were observed, yielding 10643 spectra of galaxies with $I_{AB} < 22.5$. The data were reduced by the zCOSMOS team and prepared for release in collaboration with ESO (External Data Products group/Data Products department).

We cross correlate this catalog with a morphological catalog obtained on ACS images up to $I_{AB} < 22$ in order to have both the spectroscopic redshifts and the morphological information. Details on how morphologies are obtained are described on Sect. 3.1. This ACS *I*-band catalog is part of the COSMOS HST/ACS field (Koekemoer et al. 2007). The data set consists of a contiguous 1.64 deg^2 field covering the entire COSMOS field. The Advanced Camera for Surveys (ACS) together with the *F814W* filter (“Broad *I*”) were employed.

The final catalogue contains 6240 galaxies with magnitudes ranging from $18 < I_{AB} < 22$. Since the zCOSMOS-bright catalogue is not entirely released yet, the selected sample does not have all the galaxies in this magnitude range. This is not critical if the sample is representative of all the galaxy population and no selection biases are introduced for different magnitudes. To check this point, we look at the fraction of all the $I_{AB} < 22$ mag limited sample (ACS imaging) which are selected in our sample. The selected sample represents $\sim 20\%$ of the whole sample and the selection function is basically flat at all magnitudes and for all morphologies. We therefore consider that the sample is representative of the galaxy population and unbiased.

Since we will analyze the sample properties as a function of the stellar mass, in 3.3 we will discuss the mass completeness in detail.

In this work we study galaxies in three redshift bins ($0.2 < z < 0.55$, $0.55 < z < 0.8$, $0.8 < z < 1.4$). These three bins have similar number of objects within a factor 2.

3. Physical quantities

3.1. Morphologies

The high angular resolution measured on HST images makes them ideal to properly estimate galaxy morphologies. Galaxies at low and high redshift have been historically classified by

parametric and non-parametric methods. Among the parametric methods for classifying galaxies we can mention the bulge-disc decomposition method, consisting on a 2D fit to the surface-brightness distribution of the galaxies (e.g. Trujillo et al. 2001; Aguerrí & Trujillo 2002; Peng et al. 2002; Simard et al. 2002; Trujillo & Aguerrí 2004; Aguerrí et al. 2004; de Jong et al. 2004; Aguerrí et al. 2005; Méndez-Abreu et al. 2008). On the other side, the non-parametric methods classify galaxies without any assumption on the different components of the galaxies. In this case the classification is based on some global properties of galaxies, such as color, asymmetry, or light concentration (Abraham et al. 1994; Abraham et al. 1996; van den Bergh et al. 1996). In our case, morphologies are determined in the I -band ACS images using our own developed code GALSV¹. This non-parametric N -dimensional code is based on support vector machines (SVM) and uses a training set built from a local visually classified sample. It has been tested and validated in (Huertas-Company et al. 2008). Since in this particular application the spatial resolution of the data is high, the training is built directly from the real data by performing a visual classification on a randomly selected subsample. More details on how this is performed can be consulted in Tasca et al. (2009) and Huertas-Company et al. (2009).

Basically we separate galaxies in two broad morphological types (late and early-type). By late-type we mean spiral and irregular galaxies and early-type galaxies include elliptical and lenticular types. The code gives for each galaxy a probability measure of belonging to a given morphological class. Since the classification is fully automated, we expect some errors in the classification. A visual inspection of most of the objects up to $z \sim 1$ reveals that, while the majority of the galaxies are indeed E/S0s there are some errors which increase at higher z . Most of this misclassified objects are irregular or merger galaxies with a strong starburst that produces a high concentration of light. As shown in Huertas-Company et al. (2009), the probability parameter is a good measure of the reliability of the classification; high probabilities indicating that the classification is reliable. In our case, only $\sim 5\%$ of the galaxies have associated *ambiguous* probability values between 0.4 and 0.6, so we believe our classification to be robust despite of a few misclassifications.

In the following, we decide that a galaxy belongs to a given morphological class whenever the probability is bigger than $p = 0.5$. However, in order to check the robustness of our results and the dependence on possible miss classifications, we will sometimes increase the probability threshold.

3.2. Absolute magnitudes and rest-frame color classification

We restricted the above morpho-spectroscopic $0.2 < z < 1.4$ catalogue to redshifts consistent with the photometric redshifts (Ilbert et al. 2009) to a precision of $0.1(1+z)$. This selection excludes galaxies with reliable redshifts but with a failed photometric redshift due plausible photometric problems. This final selection results in a catalogue of 6064 galaxies. Absolute (AB) magnitudes are derived using the cross-correlated spectro-photometric catalogue including the following bands; NUV-2800 Å GALEX (Zamojski et al. 2007), u^* CFHT/MegaCam and $BVg'r'i'z'$ SUBARU/SUPrime-Cam (Capak et al. 2007), K_s CFHT/WIRCam (McCracken et al. 2009), $3.6 \mu\text{m}$ and $4.5 \mu\text{m}$ SPITZER/IRAC (Sanders et al. 2007). They are optimized in a way which minimizes the dependency on the templates used to fit the multi-band photometry

¹ <http://www.lesia.obspm.fr/~huertas/galsvm.html>

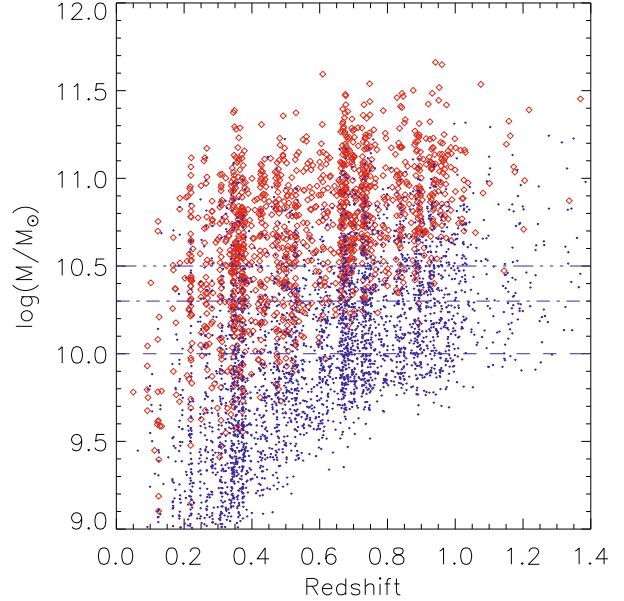


Fig. 1. Stellar mass vs. redshift. Blue points are blue late-type galaxies and red diamonds are red early-type galaxies. Horizontal lines from bottom to top show the estimated mass completeness at $z < 0.55$, $z < 0.8$ and $z < 1.4$ respectively.

(see e.g. Fig. A.1. in Ilbert et al. 2005). We use templates generated with the galaxy evolution model PEGASE.2 (Fioc & Rocca-Volmerange 1997), and the multi-band input photometry is optimized as described in Bolzonella et al. (2009).

We aim at classifying galaxies according their rest-frame colors from red to blue, and not according their PEGASE galaxy type. We applied the same technique as described in Zucca et al. (2006) with 38 templates. For this work, we consider the red galaxy subsample (templates [T1–T20]) and the blue one (templates [T21–T38]).

3.3. Stellar masses

Stellar masses are estimated from the best fitting template. In this paper, we use the estimates performed in Bolzonella et al. (2009). Since we are trying to identify trends with the stellar mass on a magnitude limited sample, it is crucial to properly understand the completeness effects. As a matter of fact, at the highest redshifts, the reddest objects will begin to drop out of the sample. Figure 1 shows the redshift of the selected objects as a function of their stellar masses. It is evident that less massive objects are not observed at high redshift, while the most massive ones are observed at all redshifts. Notice also that the blue and red galaxies have different completeness limits: blue galaxies can be observed at higher redshift than the red ones for a fixed mass. We therefore establish that our completeness limiting mass of the total sample is $\sim 5 \times 10^{10} M_*/M_\odot$ (as the mass above which red galaxies are still detected at $z \sim 1$). All galaxies with masses larger than the completeness limit can be observed at all redshifts. We can also compute the completeness mass for each of the three redshift bins, being: $\sim 10^{10} M_*/M_\odot$, $\sim 10^{10.3} M_*/M_\odot$ and $\sim 10^{10.5} M_*/M_\odot$ for galaxies located at $z < 0.55$, $z < 0.8$ and $z < 1.4$, respectively.

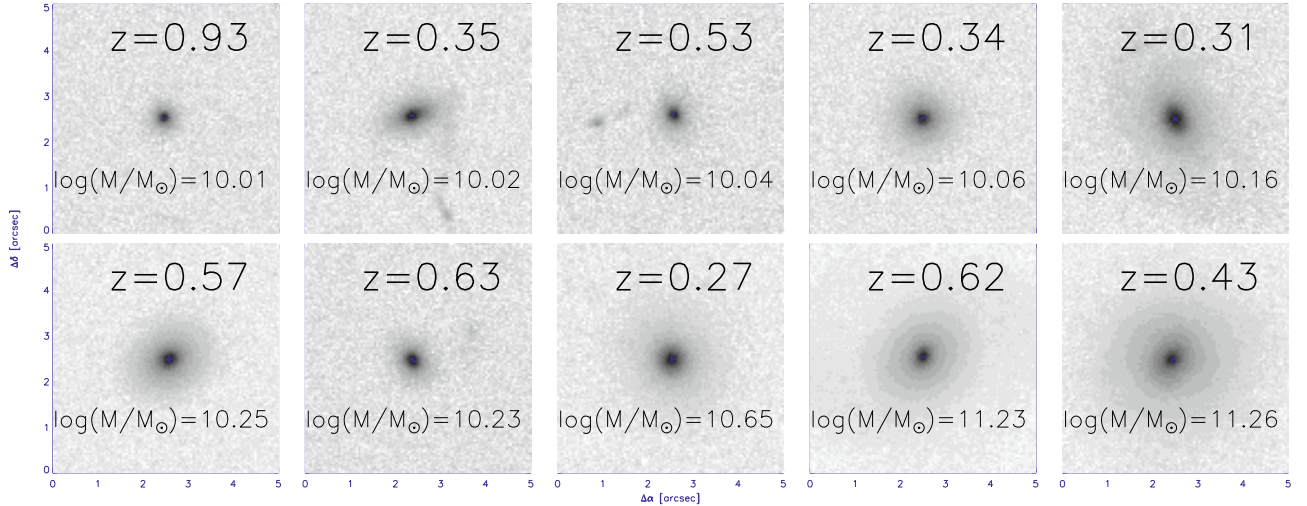


Fig. 2. $5'' \times 5''$ I -band ACS stamps of 10 blue E/S0 galaxies in our sample. Galaxies are sorted with increasing stellar mass. For each galaxy we indicate its spectroscopic redshift and its stellar mass.

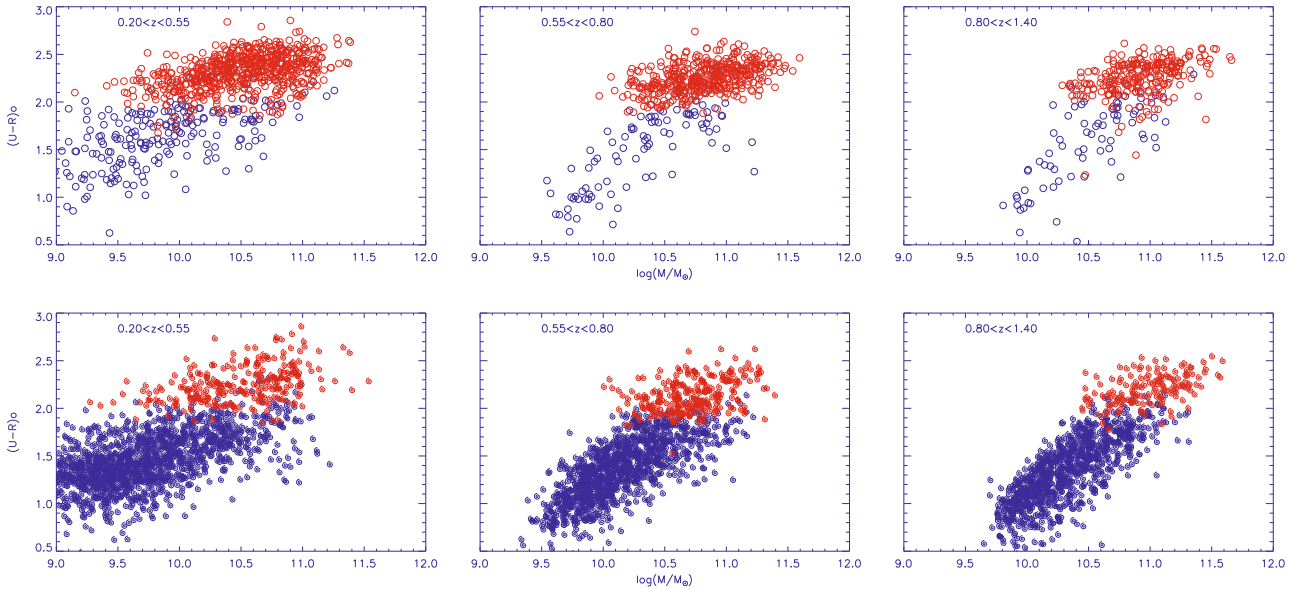


Fig. 3. $(U - R)$ rest-frame color – stellar mass diagrams for morphologically selected early-type galaxies (*top*) and late-type galaxies (*down*) in three redshift bins. Colors indicate the rest-frame color based classification: objects with red templates ([T1–T20]) are shown in red and objects with blue templates ([T21–T38]) are shown in blue.

4. Main properties of blue sequence E/S0 galaxies

4.1. Definition

We define blue early-type galaxies as galaxies with an elliptical morphology ($p > 0.5$) but which SED best fits with a blue template ([T21–T38]). As illustration, we show in Fig. 2 some ACS/HST I -band stamps of these galaxies. The majority of them appear to be symmetric and with light concentrated towards the center of the galaxy which explains why they are classified as early-type. Their SED indicates however an on-going star formation. Figure 3 indeed shows the mass color diagram for late and early-type galaxies. Notice that the blue E/S0 galaxies are located in the so-called blue cloud at the same position as normal blue spiral galaxies.

4.2. Abundance

From this section, we just consider galaxies with stellar masses above the estimated mass completeness limit at $z \sim 0.2$, i.e. galaxies with $\log(M_*/M_\odot) > 10$ to avoid effects related to the incompleteness of the sample. Using this threshold we might have some incompleteness effects in the higher redshift bins but we will properly take this into account when required. Above this mass threshold, there are 3864 galaxies between $z = 0.2$ and $z = 1.4$. Blue E/S0s represent $\sim 6\%$ of the whole sample (210 galaxies). The global morphological mixing is $\sim 46\%$ of blue late-type galaxies, $\sim 33\%$ of red E/S0s and $\sim 15\%$ red late-type galaxies which most of them are edge-on late-type systems obscured by dust (visual inspection). Globally blue early-type galaxies therefore represent a small fraction of the galaxy

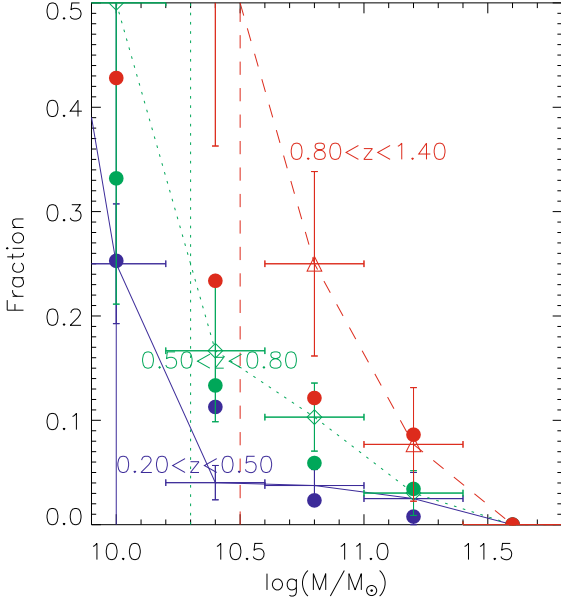


Fig. 4. Fraction of blue early-type galaxies as a function of mass at different redshifts. Red line: $0.8 < z < 1.4$, green line: $0.5 < z < 0.8$ and blue line: $0.2 < z < 0.5$. Vertical lines show the estimated mass completeness at the different redshift bins. Filled circles show the results from the Millennium simulation at all redshifts (see text for details).

distribution between $z \sim 0.2$ and $z \sim 1.4$. However, the distribution of these objects is not the same at all masses.

Kannappan et al. (2009) defined a threshold mass (M_t) at $z \sim 0$ below which the blue early-type population starts to become abundant (~ 20 – 30% of the total E/S0 population). They showed that the nature of blue E/S0 galaxies is different above and below this threshold. It appears therefore interesting to quantify this characteristic mass at high redshift to see if we detect any evolution and if it is still linked to the nature of the galaxies. Figure 4, shows the evolution of the fraction of blue ellipticals as a function of stellar mass for different redshifts. At all redshifts we do see an increase of the abundance of this population when the stellar mass decreases. We decide to perform a rough and conservative estimate of the threshold mass as the mass at which the blue early-type fraction becomes higher than 20%. Table 1 shows the measured values. The value rises from $M_t \sim 10.10 \pm 0.35$ at $z \sim 0.3$ to $M_t \sim 10.90 \pm 0.35$ at $z \sim 1$. We must nevertheless be extremely careful in analyzing these trends because of mass incompleteness effects. As a matter of fact, because of our magnitude-limited selection, red objects fall out of our sample first. Therefore, at low masses the fraction of red early-type objects might be under-estimated, causing an artificial increase of the blue fraction. Since our estimates of M_t is at all redshift bins greater than the completeness mass of the corresponding bin, we do not expect our measurements to be strongly affected by incompleteness. We also show in 4 the results from the Millennium simulations (Springel et al. 2005b) and more precisely from the Durham semi-analytical model (Bower et al. 2006; Benson et al. 2003; Cole et al. 2000). Blue E/S0s galaxies are selected as galaxies having blue colors ($U - R < 1.1$) and a bulge stellar mass greater than 80% of the total stellar mass. The color threshold is selected as the value which best divides the two bimodal peaks of the color histogram. This color threshold is different from the value one would suggest by looking at Fig. 3 which is closer to ~ 2 . This discrepancy might be explained by a difference in the magnitude system used (AB vs. Vega) or the

Table 1. Characteristic mass for different redshift bins.

	$z \sim 0$	$0.2 < z < 0.55$	$0.55 < z < 0.8$	$0.8 < z < 1.4$
$\log(M_s/M_\odot)$	11.20	11.50 ± 0.38	11.50 ± 0.58	11.50 ± 1.20
$\log(M_b/M_\odot)$	10.50	10.37 ± 0.1	10.72 ± 0.08	11.00 ± 0.2
$\log(M_t/M_\odot)$	9.70	10.10 ± 0.35	10.30 ± 0.35	10.90 ± 0.35

Notes. See text for more details on how these characteristic masses are defined. Results at $z \sim 0$ are taken from Kannappan et al. (2009).

filters sets employed. Despite of the fact that the selection criteria are not exactly the same than in our observational data, the abundance of these objects in the simulation is consistent with our measures which confirms our morphological classification and supports the fact that, at the considered stellar masses, we are not affected by incompleteness.

Another interesting mass is the bimodality mass (M_b) defined as the crossover mass between the early-type and the late-type population (e.g. Kauffmann et al. 2006). This mass is in principle not directly related to the blue E/S0 population but it is a measure of the building-up of the RS and could therefore give clues on the role of blue E/S0 galaxies in this process. Above this mass, the early-type population dominates in number over the late-type one. Several high redshift studies (e.g. Bundy et al. 2005; Pozzetti et al. 2009) have shown that this mass is evolving with look-back time becoming higher at higher redshifts. This evolution is interpreted as a signature of the downsizing assembly of galaxies. Figure 5 shows the fractions of both morphological types in the three considered redshift bins as a function of the stellar mass. At all redshifts, we do see a clear increase in number of the early-type population when the considered stellar mass is higher. Notice that at all redshifts, the turn-over mass is beyond the mass completeness limit, which means that the estimate is not affected by possible incompleteness effects. In order to properly estimate the crossover mass we perform a linear fit to the declining fraction of late-type galaxies and estimate M_b as the mass where the best fit line equals 0.5. We find this way $\log(M_b) = 10.37 \pm 0.1$ at $0.2 < z < 0.55$, $\log(M_b) = 10.72 \pm 0.08$ at $0.55 < z < 0.8$ and $\log(M_b) = 11.00 \pm 0.2$ at $0.8 < z < 1.4$. To check the robustness of these estimates with respect to the morphological classification, we repeated the measurement using increasing probability thresholds. The fluctuations of the estimated values are within the error bars. We therefore confirm the expected trend, i.e. the bimodality mass increases by 1 dex from $z \sim 0.2$ to $z \sim 1$. This reflects the fact that the red sequence is first populated with massive galaxies.

The last interesting mass is a limiting mass above which no blue galaxies are observed. This mass was defined by Kannappan et al. (2009) as the shutdown-mass (M_s). Figure 3 seem to show that this mass for blue E/S0s is close to $\sim 3 \times 10^{11} M_\odot$ at all redshifts.

4.3. Morphology

Given that the relative abundance of blue E/S0 depends on mass, it is interesting to see whether there are some differences within the blue early-type population in terms of morphology. Figure 6 shows some example stamps of blue early-type galaxies in the 3 considered redshift bins split into 2 mass bins ($M_*/M_\odot > M_t$ and $M_*/M_\odot < M_t$). Most of the blue E/S0 galaxies present regular morphologies with high central light concentration as shown in Sect. 4.1. As a general trend, massive galaxies tend to be

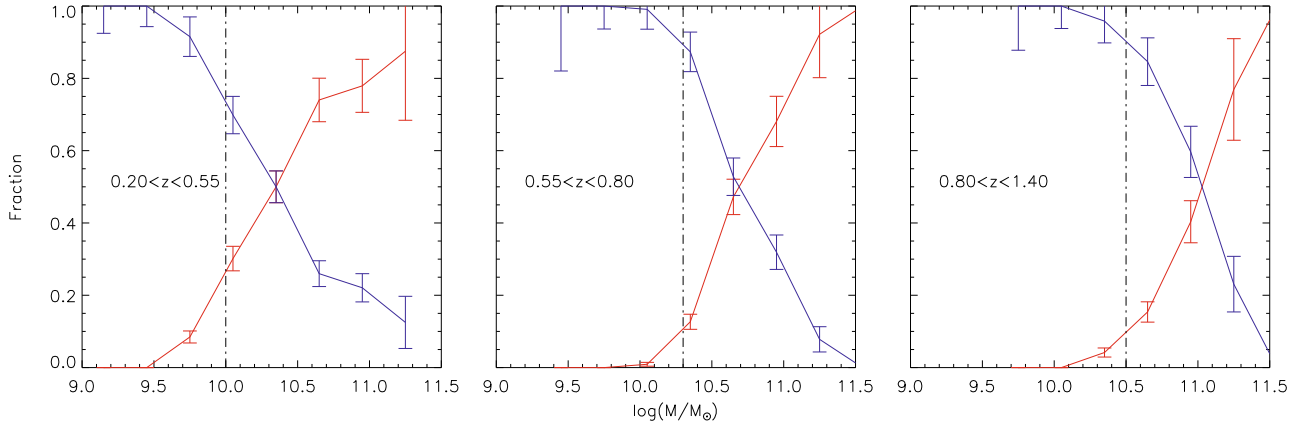


Fig. 5. Fractions of blue late-type (blue line) and red early-type galaxies (red line) in the three considered redshift bins as a function of the stellar mass. Dashed vertical lines show the estimated mass completeness at the corresponding redshift bin.

regular but with a diffuse *disky* component in the outer-parts. Less massive galaxies are more compact and it is more difficult to detect internal structures. At $z = 0$, Kannappan et al. (2009) detected in fact that less massive galaxies were more disturbed than the massive counterparts. They interpreted this as a signature of a different regime of the blue early-type population. In our case it is harder to identify this kind of details, specially in the higher redshift bin, despite the high-angular resolution delivered by HST, because of cosmological dimming effects. In the lower redshift bin however (top panel of Fig. 6) it seems that low mass blue E/S0 tend to have a higher concentration of small companions around than more massive galaxies which seem to be more isolated. Of course, we would need the redshifts of these faint companions to confirm this trend, which are not available for the moment.

4.4. Size

In Fig. 7, we plot the M_* – radius relation for blue E/S0 galaxies compared to red E/S0 and blue late-type galaxies. The r_{half} radii are computed in the *I*-band ACS images and are defined as the radius containing half of the flux of the galaxy. Globally, blue E/S0 galaxies are closer to red E/S0 than to late-type systems in the M_* – radius relation (Fig. 7) at all redshifts. We detect however some tendencies with the stellar mass. It seems that, below a given mass, blue E/S0 galaxies tend to deviate from red E/S0 in the M_* – radius plane and lie closer to normal star-forming late-type galaxies. In order to quantify this deviation we perform a linear fit to the M_* – radius of red E/S0s and compute the median distance of blue E/S0 galaxies to the best fit line as a function of mass. It rises from $\Delta r_{\text{half}}/\bar{r}_{\text{half}} \sim 0.1$ Kpc for $\log(M_*/M_\odot) > 10.5$ to $\Delta r_{\text{half}}/\bar{r}_{\text{half}} \sim 0.5$ Kpc for $\log(M_*/M_\odot) < 10.5$. The transition mass does not seem to change significantly with redshift.

4.5. Star formation

Star formation rates are estimated with the equivalent width of [OII] $\lambda 3727$ Å line measured on the publicly available zCOSMOS DR2 spectra (Lilly et al. 2009). We measure equivalent widths using our own code and transform the measured values to SFR using the relation derived in Guzman et al. (1997) (Eq. (1)).

$$SFR(M_\odot \text{ yr}^{-1}) \sim 2.5 \times 10^{-12} \times 10^{-0.4(M_B - M_{B0})} EW_{[\text{OII}]}. \quad (1)$$

Figure 8 shows the specific star formation rate (SSFR) for *normal* late-type galaxies compared to the blue early-type ones at different redshifts. We do not show the results for red early-type galaxies since very few presented [OII] emission lines. Notice also that most of the galaxies located at $0.2 < z < 0.55$ do not have measurements of their SSFR due to the [OII] emission line lies out of zCOSMOS spectral range (5000–9000 Å).

Globally the measured SSFR is comparable for both populations suggesting that blue early-type galaxies might have a disk component (either formed or in formation) which is accounting for the bulk of the star formation. Only for very massive blue-early type galaxies, above the threshold mass, we seem to detect outliers in this relation. These galaxies have indeed high specific star formation rates ($\sim 10^{-0.5} \text{ Gyr}^{-1}$) which are characteristic of a post-merger phase.

5. Discussion

5.1. Are blue E/S0 blue compact galaxies?

There is a well-known family of galaxies called blue compact galaxies. These galaxies were defined by Guzman et al. (1997) as objects presenting a high surface brightness within the half-light radius. The spectroscopic study (Phillips et al. 1997) revealed that an important fraction of these objects present emission lines characteristic of on-going star formation and hence have blue integrated colors. Our definition of blue E/S0 is different since it is based on the morphology, however we expect these galaxies to have high central light concentrations. One interesting question is therefore: are our galaxies the same blue compact galaxies? In Fig. 9 we show the *I* band magnitude versus the half light radius both computed in the ACS images. Our blue early-type galaxies indeed fall in the region of blue compact galaxies defined by Phillips et al. (1997).

There is however an important difference with respect to their work: while Phillips et al. (1997) claimed that an important fraction of these compact galaxies present blue colors, we find that the region is mostly dominated by passive early-type galaxies. This difference might be explained by incompleteness effects. They indeed used a small and deep ($I < 24$) flux limited sample and since red galaxies are lost earlier (Fig. 1), the fraction of blue galaxies in this region might be severely overestimated. In Fig. 10 we show the morphological mixing of compact galaxies in our sample as a function of the stellar mass.

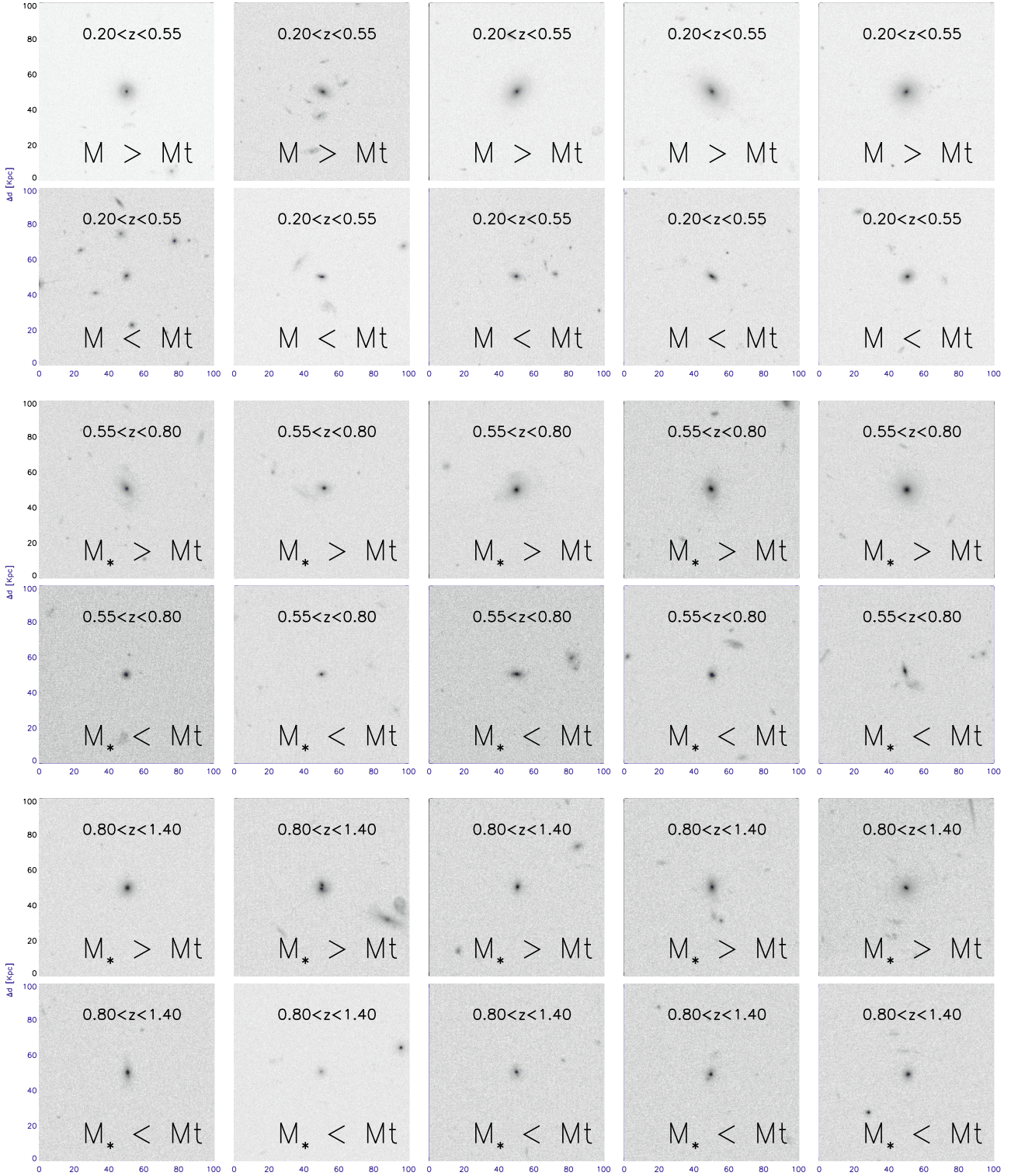


Fig. 6. ~ 100 Kpc \times 100 Kpc *I*-band ACS stamps of blue-sequence E/S0 galaxies in the three redshift bins. For illustration, we show galaxies with stellar masses greater and lower than the threshold mass at a given z .

Blue galaxies start to dominate among compact galaxies at low masses ($M_* < 10^{10} M_\odot$) where incompleteness effects in the red population become important. We argue therefore, as stated also in previous works (e.g. [Ilbert et al. 2006a](#)) that the high fraction of blue compact galaxies found in [Phillips et al. \(1997\)](#) might be biased because of the incompleteness. Indeed, their fields were deeper and covered a smaller area than ours, so their sample was

dominated by low-mass compact galaxies, while we focus here in the massive tail of the distribution.

Moreover, [Guzman et al. \(1997\)](#) concluded that most of their blue compact galaxies at high redshift (about 60%) were similar to local HII regions. We have inspected the spectral energy distribution (SED) of our blue E/S0 galaxies and conclude that they are not similar to HII galaxies. Their SEDs are similar to

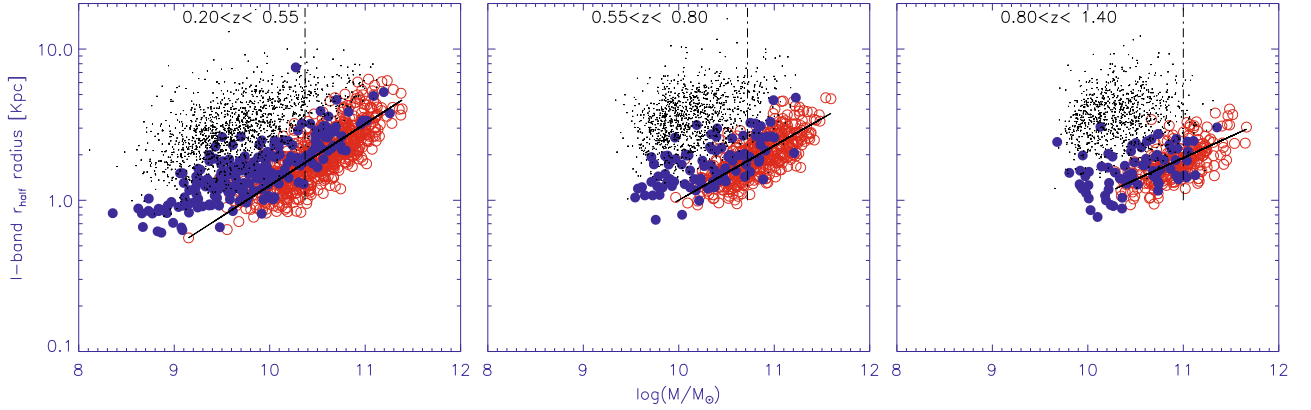


Fig. 7. Radius-stellar mass relation at different redshifts. Red circles are red E/S0 galaxies, black points are blue late-type systems and filled blue circles are blue early-type galaxies. Vertical dashed lines show the threshold mass at different redshifts as computed in Sect. 4.2. Solid line indicates the best fit line for red E/S0 galaxies.

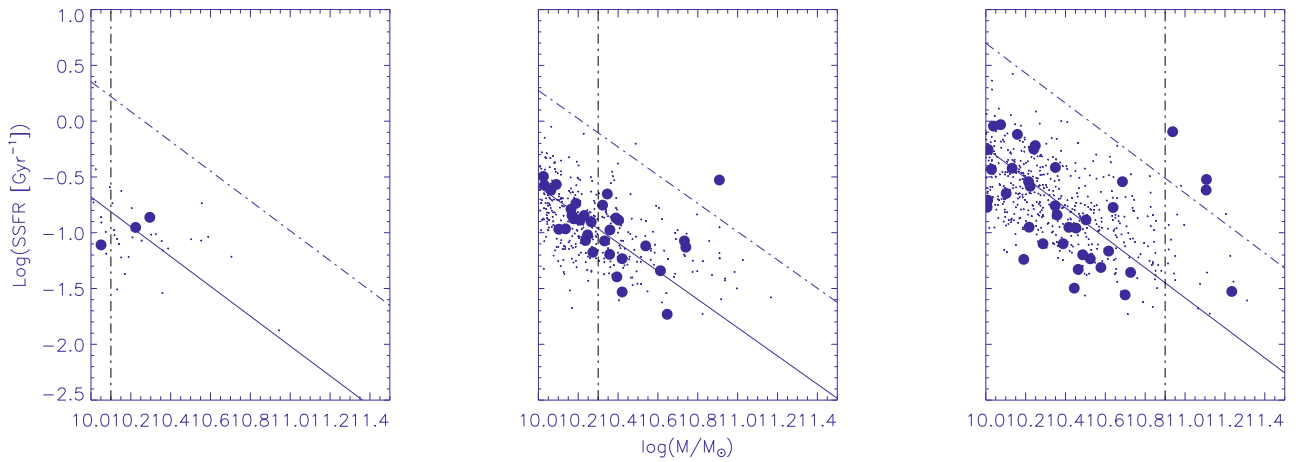


Fig. 8. Specific star formation rate as a function of stellar mass in 3 redshift bins. Black dots are normal blue late-type galaxies and blue filled dots are blue early-type galaxies. Vertical dashed lines indicate the threshold mass. Solid line is the best fit to the spiral star-forming population and dashed line is the 3-sigma limit.

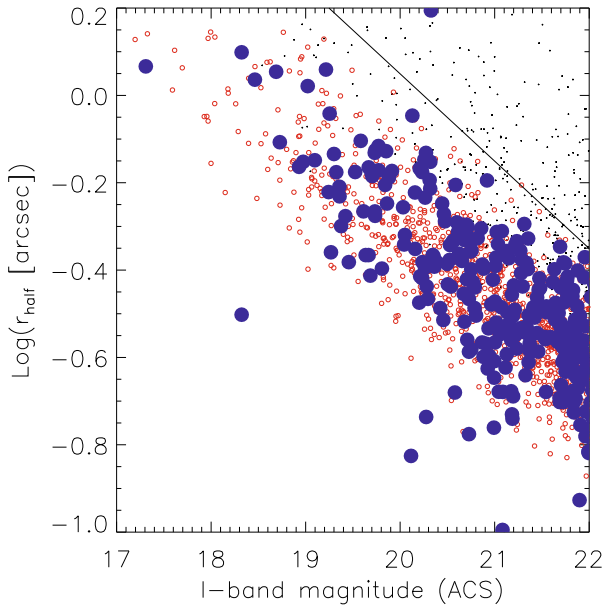


Fig. 9. I-band magnitude versus half light radius. Blue filled circles are our blue early-type galaxies, empty red circles are red E/S0 and black dots are blue late-type galaxies. The solid line shows the limit used in Phillips et al. (1997) to define compact objects.

normal starburst galaxies. We conclude that our blue E/S0 galaxies indeed are compact galaxies but are not the same population of objects as the studied in these previous works.

5.2. Characteristic masses

In Sect. 4.2 we have shown that there is no evolution of the blue E/S0 shutdown mass ($M_s \sim 3 \times 10^{11}$). This shutdown mass is indeed similar to the mass found for blue late-type galaxies. This implies that there are no blue galaxies above M_s from $z \sim 1$. It suggests that this value is not linked to the blue E/S0 population only but it is a general property of blue galaxies. This has also been found in other recent works (Cattaneo et al. 2006) and has been interpreted as a critical mass above which the blue sequence cannot exist because the gas physics is different. Only haloes below a critical shock-heating mass have gas supply by cold flows and form stars. In contrast, cooling and star formation are shut-down abruptly above this mass. Dekel & Birnboim (2006) proposed that this critical mass should be constant from $z \sim 2$ which is in agreement with our findings.

The behavior of the threshold mass is different. We have measured a decrease of ~ 1 dex from $z \sim 1$ to $z \sim 0.2$. Recently Kannappan et al. (2009) measured this threshold mass at $z \sim 0$ and found a value of $\sim 8 \times 10^9 M_\odot$. This gives a total decrease of 1.4 dex from $z \sim 1$ to $z \sim 0$. Kannappan et al. (2009) also

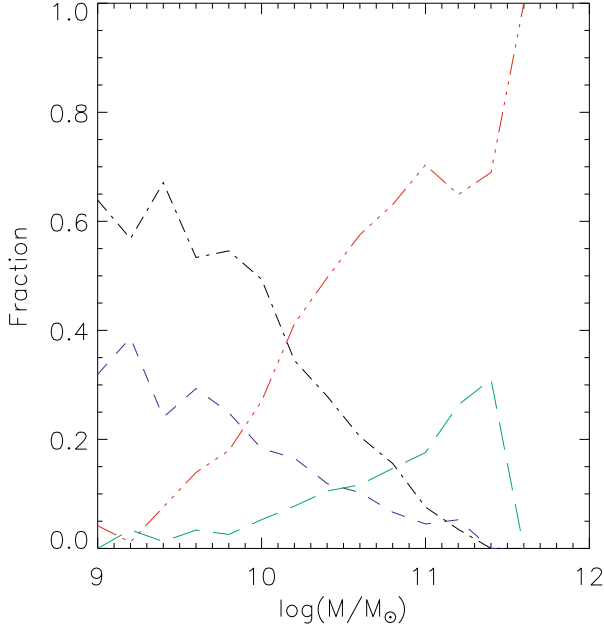


Fig. 10. Morphological mixing of compact galaxies as a function of the stellar mass. Red line are passive early-type galaxies, blue line are blue early-type galaxies, black line blue late-type galaxies and green line red late-type galaxies.

suggested that the threshold mass indicates a turnover in the dominant physical mechanisms taking place in blue E/S0 and that it should be linked to the bimodality mass. Blue E/S0 galaxies less massive than the threshold mass at $z \sim 0$ are mainly rebuilding disks while more massive galaxies are galaxies in a post-merger phase. The value they found is 1 dex smaller than the crossover mass between the passive early-type population and the star-forming late-type one in the nearby universe (bimodality mass) (Kauffmann et al. 2006) and they suggest a link between them.

Since the bimodality mass rises at high redshift (i.e. downsizing effect, Bundy et al. 2005), Kannappan et al. (2009) predicted a similar behavior for the blue E/S0 threshold mass, remaining ~ 1 dex below the bimodality mass at a given z . As shown in Sect. 4.2 M_b evolves becoming higher at higher redshifts and reflecting the fact that the building-up of the red sequence is preformed first at high masses. However, the measured values are fully compatible with the values measured for the threshold mass and we consequently do not find this expected difference between both characteristic masses. This suggests that both values are measuring the same process, i.e. the build-up of the RS. In fact, blue E/S0 start to be important in number when the RS galaxies are no longer dominant among the blue active population. We argue therefore that the bimodality mass and the threshold mass are in fact two different quantifications of the same evidence. In other words, blue early-type galaxies have a significant importance only for masses at which the RS is not yet built.

5.3. Disk rebuilding or merger remnants?

The question is now: is this bimodality-threshold mass or any other mass linked to the nature of blue E/S0 galaxies as suggested by Kannappan et al. (2009) at low z ? When looking at the SSFR at different masses (Fig. 8) we observe that all the outliers in the linear SSFR – M_* relation are located above

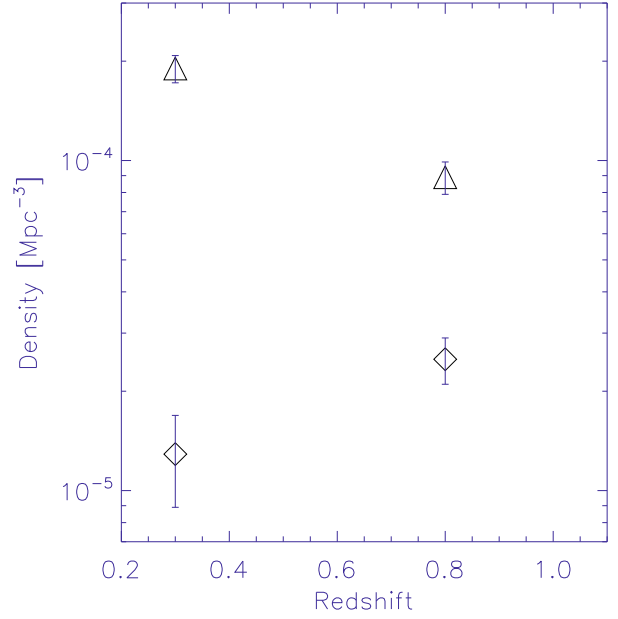


Fig. 11. Evolution of number density of blue E/S0 in two mass bins. Diamonds are blue E/S0 with $\log(M/M_\odot) > 10.8$ and triangles are blue E/S0 with $10 < \log(M/M_\odot) < 10.8$.

$\log(M_*/M_\odot) \sim 10.8$ at all redshifts which is bigger than the threshold mass (M_t): above this mass, blue E/S0 tend to have higher specific star formation rates ($> 10^{-0.5} \text{ Gyr}^{-1}$). By definition, the number of galaxies above M_t is small so it becomes difficult to establish robust conclusions but we can affirm that all the outliers fall above $\log(M_*/M_\odot) \sim 10.8$. This result suggests indeed that there might be a change in the physical processes taking place in blue E/S0 depending on the mass. This high SSFR is in fact characteristic of strong starburst (e.g. Springel et al. 2005b) and these objects could be galaxies experiencing a violent episode of star formation in a post merger phase. Their normal evolution would therefore be a migration to the RS after consumption of the available gas. This later affirmation is also supported by the $r_{\text{half}} - M_*$ relation in which we can see that massive blue E/S0 galaxies tend to fall within the same region as passive red E/S0s at all redshifts (Fig. 7). The visual inspection of these massive galaxies (Figs. 2 and 6) does not reveal important perturbations up to our resolution limit, suggesting that these galaxies have already acquired their early-type morphology and are ready to migrate into the RS. Moreover, they seem to lie in low density environments or at least not close to comparable mass companions (Figs. 2 and 6) which seems to indicate that they will probably not experience a major merger event in the next Gyr.

According to numerical simulations of mergers of massive gas-rich galaxies, the typical time scale to move from the blue cloud to the RS after a major merger event is $\sim 2-3$ Gyr (Springel et al. 2005b). Consequently, if the most massive blue E/S0 galaxies were indeed galaxies in a post-merger phase, we could expect a decrease of the density of these objects in this time interval since we expect a decrease in the merger rate with cosmic time (e.g. Conselice et al. 2009, 2008; Le Fèvre et al. 2000). In order to check this, we have computed the number density of blue E/S0 galaxies in two redshift bins of 3 Gyr each ($0.2 < z < 0.55$ and $0.55 < z < 1.4$) for two mass regimes. In Fig. 11 we see that the comoving number density of the most massive blue E/S0 galaxies ($\log(M/M_\odot) > 10.8$) decreases from $z \sim 0.8$ to

$z \sim 0.1$ of a factor ~ 2 . This suggests that these galaxies have time to move to the RS in less than 3 Gyr, as expected from major merger remnants.

At lower masses ($\log(M_*/M_\odot) < 10.8$) however, the SSFR of blue E/S0 is similar to the one of star-forming late type galaxies (Fig. 8) suggesting that these galaxies are more similar to normal disks. Moreover, if we look at the $r_{\text{half}} - M_*$ relation (Fig. 7) we do see that these galaxies start to deviate from the relation of passive E/S0 and lie between the late-type and the early-type zone. They are consequently smaller than normal rotating disks at the same redshift but larger than spheroids. This suggests that these galaxies might evolve differently than their massive counter-parts. In any case, the main driver of their evolution should have time scales larger than 3 Gyr since we do not observe a decrease in their number density in this time interval (see Fig. 11). Our guess is that 1) they can evolve by fading until becoming normal disks; 2) they can be rebuilding disks from surrounding gas (Governato et al. 2007; Robertson & Bullock 2008) as suggested by Hammer et al. (2001) or 3) they can have built a bulge component through minor mergers and be in a reddening phase or *morphological quenching* phase as proposed by Martig et al. (2009). The last two hypothesis require gas accretion: in this case where is the gas coming from? It does not seem that the presence of gas is a consequence of a major merger event since we do not detect any outlier in the SSFR - M_* relation and disk rebuilding after a major merger event can be done in a relatively short time scale (Hammer et al. 2009). It is more likely that these galaxies are the result of minor mergers which triggered the star formation in the central parts (Aguerre et al. 2001; Eliche-Moral et al. 2006) and built a bulge component (Martig et al. 2009). This process would also imply a disk growth since most of the satellites mass is expected to fall in the outer parts. Even if the analysis of their environment reveals that the majority of them do not lie in dense environments up our completeness limit, all blue E/S0 galaxies lying in relatively high environments ($D3 > 0.1$) have low masses and we cannot reject the possibility that they might have gas-rich low-mass companions as we seem to detect in the ACS images. If this scenario revealed to be true, according to the numerical simulations performed by Martig et al. (2009), these galaxies then will redden in $\sim 4-5$ Gyr between $z \sim 1$ and $z \sim 0.2$ through what they called a *morphological quenching* phase.

In order to investigate further the future of these objects and in particular the fading scenario for the less massive galaxies, we compare in Fig. 12 the surface brightness - mass relation of our objects with local galaxies from the SDSS DR4 (Adelman-McCarthy et al. 2006) and more precisely from the *low redshift* catalog described in Blanton et al. (2005). We define a local galaxy to be early-type or late-type based on the Sersic index computed by Blanton et al. (2005). This definition is slightly different than the one used for the high-redshift sample but we do not expect the differences to be significant since there is a very tight relation between the Sersic index and the visual morphology at low redshift. The surface brightness is computed in the r rest-frame band in both samples to avoid wavelength dependent effects. Massive blue early-type galaxies at high redshift overlap with the zone of local passive early-type galaxies, indicating that they will probably transform into this class. However, less massive galaxies lie in a different zone which has no local counter part, suggesting that they are experiencing strong evolution. In order to reach the local star-forming region a fading of ~ 2 mag in the r band is required. Nevertheless, even if E/S0 blue galaxies could suffer this fading, the resulting spiral galaxies would be smaller than the observed normal spirals

galaxies in the nearby Universe. As a matter of fact, we do not expect a large increment of the scale for a late-type galaxy evolving just by pure passive evolution (see Trujillo & Aguerri 2004; Brook et al. 2006; Kanwar et al. 2008; Azzollini et al. 2008). In contrast the (re)building of the outermost regions of the galaxies by the accretion of gas would increase the mass and size of the galaxies moving E/S0 blue objects to the positions occupied by normal local galaxies in the surface brightness-mass plane.

6. Summary and conclusions

We have studied some of the properties of a population of 210 blue early-type galaxies with $M_*/M_\odot > 10^{10}$ from $z \sim 1$ in the COSMOS field. Our sample is complete up to $M_*/M_\odot \sim 10^{10}$ in the lower redshift bin and the completeness limit rises to $M_*/M_\odot \sim 5 \times 10^{10}$ at $z \sim 1$. Spectroscopic redshifts come from the zCOSMOS 10k release. Morphologies are determined in the ACS images using our tested and validated code GALSVM and the spectral classification is performed using a best-fitting technique with 38 templates on the primary photometric COSMOS catalogues. We define a blue E/S0 galaxy as an object presenting an early-type morphology and which SED best fits with a blue template.

The main properties of these galaxies summarize as follows:

- Globally blue E/S0 galaxies represent $\sim 5\%$ of the whole sample of early-type galaxies with $M_*/M_\odot > 10^{10}$ from $z \sim 1.4$. Nevertheless the abundance strongly depends on the considered stellar mass. Below a threshold mass (M_t), they become more abundant and represent about 20% of the red early-type population. This threshold mass evolves with redshift from $M_t \sim 11.1$ at $z \sim 1$ to $M_t \sim 10.1$ at $z \sim 0.2$. This evolution matches the evolution of the bimodality mass (crossover mass between late-type blue population and the early-type red population). Both masses are therefore a measure of the build-up of the RS. In contrast, the shutdown mass (mass above which blue galaxies disappear) does not evolve. This could be related with differences in the gas physics above a critical mass.
- Blue E/S0 galaxies fall in the same region in the magnitude-radius space than blue compact galaxies defined by Guzman et al. (1997). However it is not the same population since we focus here in the massive tail of the distribution which is dominated by passive red E/S0 galaxies.
- The visual inspection of these galaxies does not reveal important perturbations up to our resolution limit. On the contrary, galaxies seem to have a well-defined shape with high-central light concentration. Low mass galaxies seem to have more small companions than the massive counter-parts, however we do not have spectroscopic information to confirm this trend.
- Massive blue E/S0 ($\log M_*/M_\odot > 10.5$) galaxies tend to have similar sizes than E/S0 galaxies. At lower masses however they tend to lie between spirals and spheroids.
- The specific star formation rate measured with the [OII]3727 line and stellar masses, shows that blue E/S0 galaxies have similar SSFR values than normal star-forming spirals. The outliers of this relation are galaxies more massive than $\log(M_*/M_\odot) \sim 10.8$. These outliers present SSFR characteristic of post-merger galaxies ($\sim 10^{2.5} \text{ Gyr}^{-1}$).

These results seem to point out that these galaxies have different natures depending on their stellar mass. Massive objects

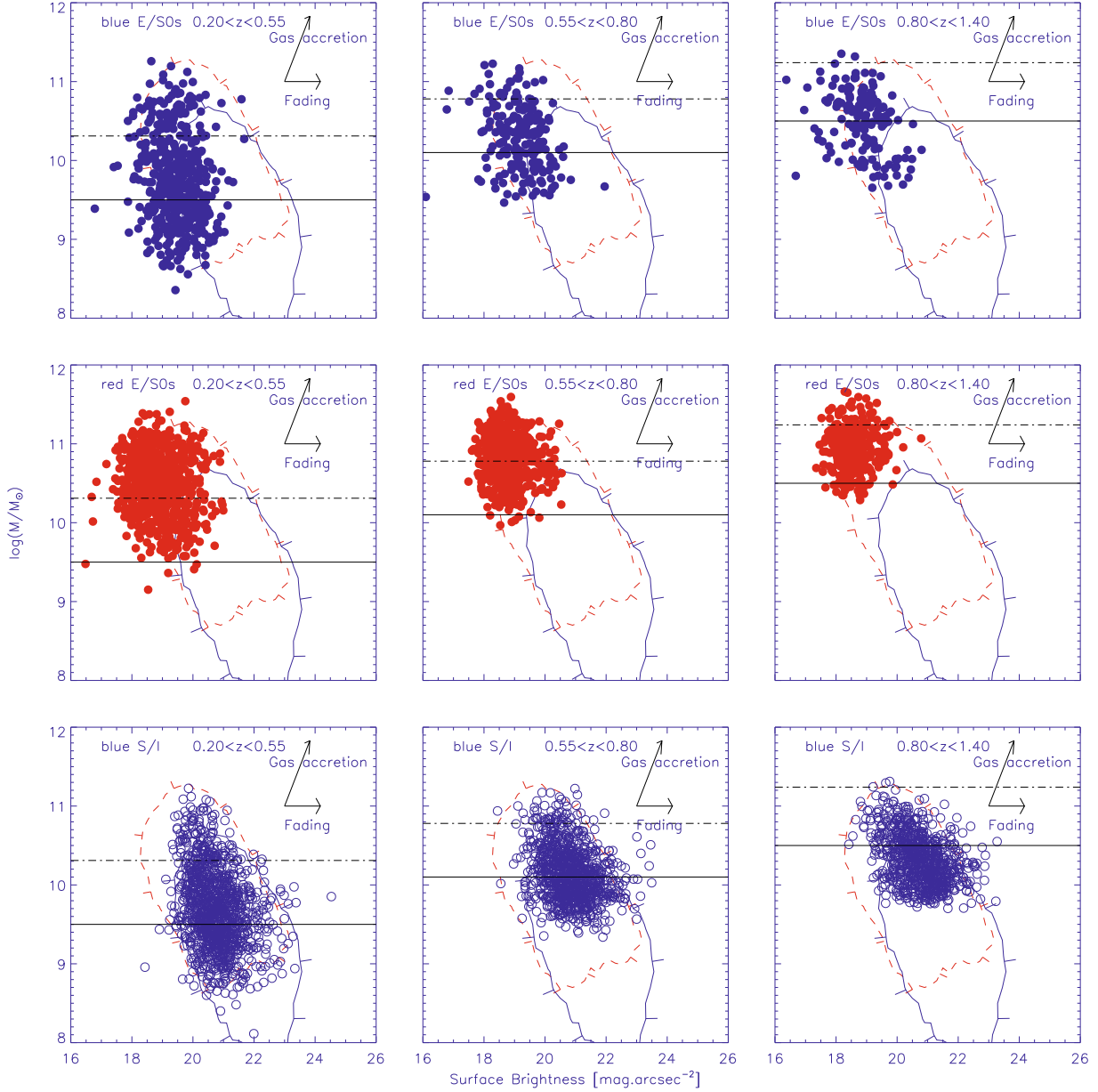


Fig. 12. R -band rest-frame surface brightness vs. stellar mass for our sample compared with the SDSS DR4 sample. Each column shows a different redshift range, i.e. from left to right: $0.2 < z < 0.55$, $0.55 < z < 0.8$ and $0.8 < z < 1.4$. Contours show in all sub-figures the location (20 galaxies iso-contour) of local galaxies (red dashed contours are early-type galaxies and blue solid contours are late-type galaxies). Over plotted are galaxies in our sample, *top*: blue E/S0, *middle*: red E/S0, and *bottom*: blue late-type systems. Dashed horizontal lines indicate the threshold mass and the solid line are our completeness limit. Arrows show typical movements in the plane caused by fading or disk rebuilding activity.

($\log(M_*/M_\odot) > 10.8$), are probably post mergers galaxies migrating to the red sequence while less massive galaxies are more likely progenitors of today's late-type galaxies which are accreting gas. The migration of the massive galaxies is faster than 3 Gyr as expected by numerical simulations of merger remnants. Indeed, the evolution of the number density computed in redshift bins of equal time show that the most massive E/S0 galaxies evolved in typical time scales smaller than 3 Gyr. In contrast the evolution of blue early-type galaxies with smaller masses is produced in larger time scales. This low-mass galaxies might be the result of minor-mergers with surrounding satellites which triggered the central star formation and built-up a bulge component, and therefore appear with an early-type shape.

The confirmation of these hypothesis requires a detailed analysis of the internal kinematics of these objects to see if the

physics is indeed different. In particular, 3D spectroscopy should be useful to get more details about their nature.

Acknowledgements. Based on zCOSMOS observations carried out using the Very Large Telescope at the ESO Paranal Observatory under Programme ID: LP175.A-0839. The Millennium Simulation databases used in this paper and the web application providing online access to them were constructed as part of the activities of the German Astrophysical Virtual Observatory. The authors would like to thank ESO for financial support.

References

- Abraham, R., van den Bergh, S., Glazebrook, K., et al. 1996, *ApJS*, 107, 1
- Abraham, R. G., Valdes, F., Yee, H. K. C., & van den Bergh, S. 1994, *ApJ*, 432, 75
- Adelman-McCarthy, J. K., Agüeros, M. A., Allam, S. S., et al. 2006, *ApJS*, 162, 38

- Aguerri, J. A. L., & Trujillo, I. 2002, *MNRAS*, 333, 633
- Aguerri, J. A. L., Balcells, M., & Peletier, R. F. 2001, *A&A*, 367, 428
- Aguerri, J. A. L., Iglesias-Paramo, J., Vilchez, J. M., & Muñoz-Tuñón, C. 2004, *AJ*, 127, 1344
- Aguerri, J. A. L., Iglesias-Paramo, J., Vilchez, J. M., Muñoz-Tuñón, C., & Sánchez-Janssen, R. 2005, *AJ*, 130, 475
- Azzollini, R., Trujillo, I., & Beckman, J. E. 2008, *ApJ*, 684, 1026
- Baldry, I. K., Glazebrook, K., Brinkmann, J., et al. 2004, *ApJ*, 600, 681
- Bamford, S. P., Nichol, R. C., Baldry, I. K., et al. 2009, *MNRAS*, 393, 1324
- Barnes, J. E. 2002, *MNRAS*, 333, 481
- Benson, A. J., Bower, R. G., Frenk, C. S., et al. 2003, *ApJ*, 599, 38
- Binney, J. 1977, *ApJ*, 215, 483
- Blanton, M. R., Schlegel, D. J., Strauss, M. A., et al. 2005, *AJ*, 129, 2562
- Blumenthal, G. R., Faber, S. M., Primack, J. R., & Rees, M. J. 1984, *Nature*, 311, 517
- Bolzonella, M., Kovac, K., Pozzetti, L., et al. 2009, *A&A*, submitted [arXiv:0907.0013]
- Bower, R. G., Benson, A. J., Malbon, R., et al. 2006, *MNRAS*, 370, 645
- Brook, C. B., Kawata, D., Martel, H., Gibson, B. K., & Bailin, J. 2006, *ApJ*, 639, 126
- Bundy, K., Ellis, R. S., & Conselice, C. J. 2005, *ApJ*, 625, 621
- Capak, P., Aussel, H., Ajiki, M., et al. 2007, *ApJS*, 172, 99
- Cattaneo, A., Dekel, A., Devriendt, J., Guiderdoni, B., & Blaizot, J. 2006, *MNRAS*, 370, 1651
- Cattaneo, A., Dekel, A., Faber, S. M., & Guiderdoni, B. 2008, *MNRAS*, 389, 567
- Cimatti, A., Daddi, E., & Renzini, A. 2006, *A&A*, 453, L29
- Cole, S., Lacey, C. G., Baugh, C. M., & Frenk, C. S. 2000, *MNRAS*, 319, 168
- Conselice, C. J., Rajgor, S., & Myers, R. 2008, *MNRAS*, 386, 909
- Conselice, C. J., Yang, C., & Bluck, A. F. L. 2009, *MNRAS*, 394, 1956
- Cowie, L. L., Songaila, A., Hu, E. M., & Cohen, J. G. 1996, *AJ*, 112, 839
- Cox, T. J., Primack, J., Jonsson, P., & Somerville, R. S. 2004, *ApJ*, 607, L87
- de Jong, R. S., Simard, L., Davies, R. L., et al. 2004, *MNRAS*, 355, 1155
- De Lucia, G., Springel, V., White, S. D. M., Croton, D., & Kauffmann, G. 2006, *MNRAS*, 366, 499
- Dekel, A., & Birnboim, Y. 2006, *MNRAS*, 368, 2
- Eliche-Moral, M. C., Balcells, M., Aguerri, J. A. L., & González-García, A. C. 2006, *A&A*, 457, 91
- Faber, S. M., Willmer, C. N. A., Wolf, C., et al. 2007, *ApJ*, 665, 265
- Fabian, A. C. 1999, *MNRAS*, 308, L39
- Ferreras, I., Lisker, T., Pasquali, A., & Kaviraj, S. 2009, *MNRAS*, 395, 554
- Governato, F., Willman, B., Mayer, L., et al. 2007, *MNRAS*, 374, 1479
- Guzman, R., Gallego, J., Koo, D. C., et al. 1997, *ApJ*, 489, 559
- Hammer, F., Gruel, N., Thuan, T. X., Flores, H., & Infante, L. 2001, *ApJ*, 550, 570
- Hammer, F., Flores, H., Yang, Y. B., et al. 2009, *A&A*, 496, 381
- Hernquist, L., & Mihos, J. C. 1995, *ApJ*, 448, 41
- Huertas-Company, M., Rouan, D., Tasca, L., Soucail, G., & Le Fèvre, O. 2008, *A&A*, 478, 971
- Huertas-Company, M., Tasca, L., Rouan, D., et al. 2009, *A&A*, 497, 743
- Ilbert, O., Arnouts, S., McCracken, H. J., et al. 2006a, *A&A*, 457, 841
- Ilbert, O., Lauger, S., Tresse, L., et al. 2006b, *A&A*, 453, 809
- Kannappan, S. J. 2004, *ApJ*, 611, L89
- Kannappan, S. J., & Wei, L. H. 2008, in *The Evolution of Galaxies Through the Neutral Hydrogen Window*, ed. R. Minchin, & E. Momjian, *Am. Inst. Phys. Conf. Ser.*, 1035, 163
- Kannappan, S. J., Guie, J. M., & Baker, A. J. 2009, *AJ*, 138, 579
- Kanwar, A., Simard, L., Schade, D., & Gwyn, S. D. J. 2008, *ApJ*, 682, 907
- Kauffmann, G., Heckman, T. M., De Lucia, G., et al. 2006, *MNRAS*, 367, 1394
- Kereš, D., Katz, N., Weinberg, D. H., & Davé, R. 2005, *MNRAS*, 363, 2
- King, A. 2003, *ApJ*, 596, L27
- Koekemoer, A. M., Aussel, H., Calzetti, D., et al. 2007, *ApJS*, 172, 196
- Le Fèvre, O., Abraham, R., Lilly, S. J., et al. 2000, *MNRAS*, 311, 565
- Lilly, S. J., LeBrun, V., Maier, C., et al. 2009, *ApJS*, 184, 218
- Martig, M., Bournaud, F., Teyssier, R., & Dekel, A. 2009, *ApJ*, 707, 250
- Méndez-Abreu, J., Aguerri, J. A. L., Corsini, E. M., & Simonneau, E. 2008, *A&A*, 487, 555
- Mihos, J. C., & Hernquist, L. 1996, *ApJ*, 464, 641
- Peng, C. Y., Ho, L. C., Impey, C. D., & Rix, H.-W. 2002, *AJ*, 124, 266
- Phillips, A. C., Guzman, R., Gallego, J., et al. 1997, *ApJ*, 489, 543
- Pozzetti, L., Bolzonella, M., Zucca, E., et al. 2009, *A&A*, submitted [arXiv:0907.5416]
- Puech, M., Hammer, F., Lehnert, M. D., & Flores, H. 2007, *A&A*, 466, 83
- Rees, M. J., & Ostriker, J. P. 1977, *MNRAS*, 179, 541
- Robertson, B. E., & Bullock, J. S. 2008, *ApJ*, 685, L27
- Sanders, D. B., Salvato, M., Aussel, H., et al. 2007, *ApJS*, 172, 86
- Schawinski, K., Lintott, C., Thomas, D., et al. 2009, *MNRAS*, 396, 818
- Scoville, N., Aussel, H., Brusa, M., et al. 2007, *ApJS*, 172, 1
- Silk, J., & Rees, M. J. 1998, *A&A*, 331, L1
- Simard, L., Willmer, C. N. A., Vogt, N. P., et al. 2002, *ApJS*, 142, 1
- Springel, V., Di Matteo, T., & Hernquist, L. 2005a, *ApJ*, 620, L79
- Springel, V., White, S. D. M., Jenkins, A., et al. 2005b, *Nature*, 435, 629
- Strateva, I., Ivezić, Ž., Knapp, G. R., et al. 2001, *AJ*, 122, 1861
- Tasca, L. A. M., Kneib, J., Iovino, A., et al. 2009, *A&A*, 503, 379
- Trujillo, I., & Aguerri, J. A. L. 2004, *MNRAS*, 355, 82
- Trujillo, I., Graham, A. W., & Caon, N. 2001, *MNRAS*, 326, 869
- van den Bergh, S., Abraham, R. G., Ellis, R. S., et al. 1996, *AJ*, 112, 359
- White, S. D. M., & Rees, M. J. 1978, *MNRAS*, 183, 341
- Wyithe, J. S. B., & Loeb, A. 2003, *ApJ*, 595, 614
- Zamojski, M. A., Schiminovich, D., Rich, R. M., et al. 2007, *ApJS*, 172, 468